Mine Water and the Environment (2022) 41:5–15
https://doi.org/10.1007/s10230-021-00836-5

TECHNICAL ARTICLE

Antimony Mobilisation and Attenuation During Ore Processing at Orogenic Gold Mines, Southern New Zealand

E. Weightman[1] · D. Craw[1] · T. Snow[2] · G. Kerr[1]

Received: 1 October 2020 / Accepted: 5 November 2021 / Published online: 21 November 2021

Abstract

Mine waters at the Reefton orogenic gold mine (active from 2007 to 2016) in southern New Zealand contained dissolved arsenic (As) and antimony (Sb) up to 5 mg/L during production of a sulfide concentrate that included arsenopyrite (FeAsS) and stibnite (Sb_2S_3). Ferric oxyhydroxide adsorption extracted As down to < 0.1 mg/L but dissolved Sb remained elevated due to adsorption competition with As. The Reefton sulfide concentrate was transported 700 km to the Macraes orogenic gold mine (active from 1990) for processing through a pressure oxidation autoclave at 225 °C. The Macraes ore has low Sb contents, so the temporary introduction of a Sb-rich component produced a short-term Sb signal in the autoclave system and tailings waters. Oxidation of stibnite occurred rapidly in the autoclave, in parallel with the As in the arsenopyrite, producing ferric antimonate (tentatively identified as As-bearing tripuhyite) and ferric arsenate ($FeAsO_4$). Dissolved Sb in the Macraes tailings waters remained < 0.1 mg/L throughout the period of Reefton concentrate addition. The formation of tripuhyite in the high-temperature autoclave stabilised Sb in the Macraes tailings, so that dissolved Sb < As, in contrast to the low-temperature processes at Reefton where dissolved Sb > As.

Keywords Tripuhyite · Autoclave · Oxidation · Tailings · Arsenic · Adsorption

Introduction

Arsenic (As) is well-known as a potentially toxic metalloid that can be present at elevated concentrations around mines, especially orogenic gold mines (Bowell and Craw 2014; Majzlan et al. 2011; Ritchie et al. 2013). Consequently, the geochemical and environmental behaviour of As is generally well understood, as are the minerals that can control As in the environment (Bowell 1994; Bowell and Craw 2014; Jain et al. 1999; Langmuir et al. 2006; Majzlan et al. 2011, 2015; Riveros et al. 2001). Antimony (Sb) commonly accompanies As at mine sites (Ashley et al. 2003; Druzbicka and Craw 2015; Majzlan et al. 2011; Ritchie et al. 2013), and laboratory experiments on attenuation of As and Sb and possible competition between these metalloids for adsorption sites, have been conducted to predict processes affecting water quality (e.g. Guo et al. 2014; McComb et al. 2007; Muller et al. 2015; Roddick-Lanzilotta et al. 2002; Swedlund et al. 2015; Vithanage et al. 2013; Waychunas et al. 1993). However, the geochemical behaviour and mineralogical constraints on Sb mobility, especially, at mine sites, are less well understood and are the subjects of on-going research (Druzbicka and Craw 2015; Fawcett et al. 2015; Filella et al. 2009; Guo et al. 2014; Leverett et al. 2012; Maher 2009; Majzlan et al. 2016; Radkova et al. 2017, 2020). This paper examines the mobilisation and attenuation of As and Sb at the large scales of open cut mines over decadal time scales, in contrasting climatic regimes, and compares these observations to previously determined laboratory experiments.

Gold extraction at mines can be limited by so-called refractory ore, in which micron-scale gold particles are encapsulated in sulfide mineral grains (Kerr et al. 2015a; Paktunc et al. 2013). One way to address this processing problem is to oxidise the sulfide minerals and liberate the gold. This can be done efficiently in a pressure oxidation system (Fleming 2010; Kerr et al. 2015a; La Brooy et al. 1994). Since the sulfide minerals host most of the As and Sb in the ore, this process also oxidises and liberates the metalloids with iron oxyhydroxide (HFO) and jarosite (Craw

✉ D. Craw
dave.craw@otago.ac.nz

[1] Geology Department, University of Otago, PO Box 56, Dunedin 9054, New Zealand

[2] Oceana Gold Ltd, Macraes Flat, East Otago, New Zealand

2006; Kerr et al. 2015a; Langmuir et al. 2006; Paktunc et al. 2013). There has been abundant research on the transformations of As in this process, and the environmental stability of that As in discarded tailings has been assessed (Bowell and Craw 2014; Kerr et al. 2015a; Langmuir et al. 2006; Paktunc et al., 2013; Riveros et al. 2001). However, the response of Sb to pressure oxidation has received less attention and the environmental stability of Sb in the HFO- and jarosite-bearing tailings is not well known (e.g. Karimian et al. 2017; Leverett et al. 2012; Multani et al. 2017).

In this study, we address the issues of Sb-bearing ore during processing, pressure oxidation, and subsequent disposal into tailings for long-term storage at the Reefton and Macraes orogenic gold mines in southern New Zealand (Fig. 1a–c). The Macraes deposit (Fig. 1b) has only low levels of Sb in the ore: < 50 mg/kg in bulk ore, and up to 2000 mg/kg in solid solution in arsenopyrite (Craw and MacKenzie 2016). However, additional Sb-bearing sulfide concentrate (≈ 4000 mg/kg Sb) was transported for nine years from the Reefton mine (Fig. 1a, c; Milham and Craw 2009) to the Macraes mine for processing in the Macraes pressure oxidation system, and monitoring of metalloid concentrations in waters from both mines was carried out over that time. Consequently, we can contrast the mobility of Sb, along with As, in mine waters in the Reefton and Macraes processing systems. Mine water metalloid concentrations at both sites in the initial stages of this mining activity were documented by Milham and Craw (2009); this study now extends the metalloid mobility evaluation over a longer time scale. In particular, we focus on Sb in the Macraes pressure oxidation system in the transition from processing Sb-bearing concentrate to the subsequent absence of Sb-bearing concentrate, and on the coeval Sb concentrations in the tailings waters.

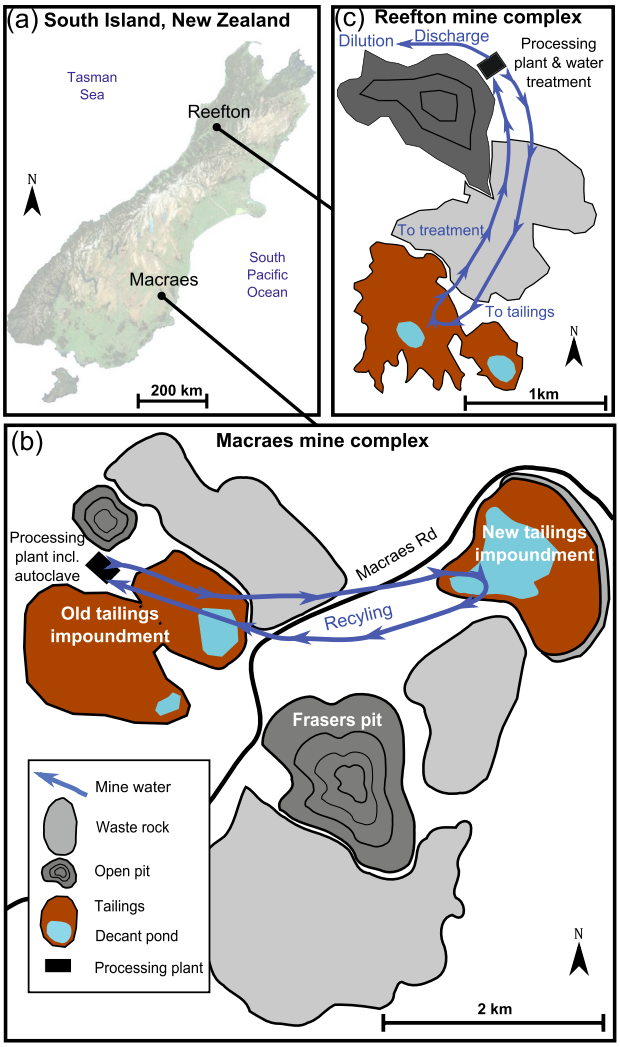

Fig. 1 Location maps for the mine sites described in this study. **a** Locations of the sites on opposite sides of the South Island, New Zealand. **b** Macraes mine site. **c** Reefton mine site

General Setting

Mine Sites

The Macraes gold mine extracts gold from an orogenic gold deposit hosted in the Mesozoic Otago Schist belt in New Zealand's South Island (Fig. 1a, b; Craw and MacKenzie 2016). The deposit is hosted in a shear zone, with relatively little quartz veining, and the total resource is ≈ 370 t (12 Moz) Au at ≈ 1 g/t, of which 155 t (5 Moz) have been extracted since the modern mine opened in 1990 (Craw and MacKenzie 2016). Most of the gold is encapsulated in arsenopyrite and pyrite, which constitute as little as 0.2–0.4% of the disseminated ore, so sulfides are concentrated up to 40-fold through flotation to form an ore concentrate with 8–10% S before passing through a pressure oxidation autoclave (Fig. 2a,b; Craw 2006; Kerr et al. 2015a).

Paleozoic orogenic systems near Reefton (Fig. 1a, c) involved two phases of mineralisation: early quartz veins with Au-bearing pyrite and arsenopyrite; and a later event which introduced stibnite along with further Au-bearing pyrite and arsenopyrite during shear deformation (Kerr et al. 2015b; Milham and Craw 2009). Open pit mines at Reefton operated from 2007 to 2016, and sulfide concentrates were transported 700 km to Macraes for further processing (Milham and Craw 2009). The concentrates, with ≈ 22% S, were formed via flotation and the tailings discarded in a large impoundment (Fig. 1c). Sulfide concentrates contained up to 4% stibnite along with several percent each of pyrite and arsenopyrite, and the arsenopyrite included up to 1000 mg/kg Sb in solid solution (Milham and Craw 2009).

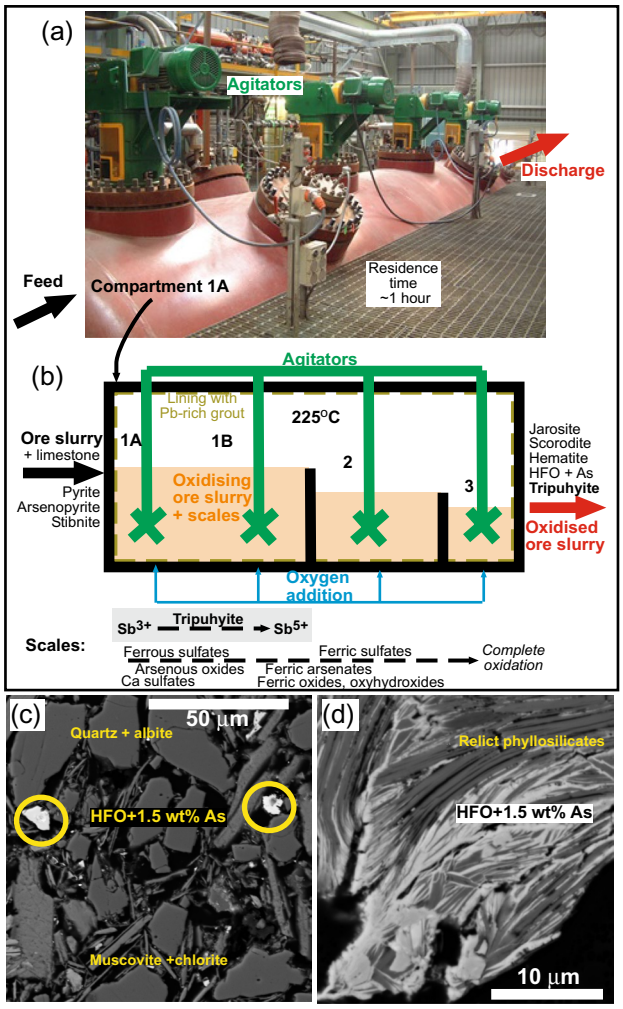

Fig. 2 Pressure oxidation processes and products at the Macraes mine. **a** Photograph of the autoclave. **b** Sketch of the internal structure of the autoclave, with principal minerals that form in the oxidising ore slurry and scales. **c** SEM image of tailings that are dominated by silicates from flotation, with minor autoclave discharge components (white). **d** Close view of an autoclave tailings particle composed of degraded phyllosilicate coated by As-bearing HFO

Pressure Oxidation

The pressure oxidation autoclave at Macraes is used to rapidly oxidise the ore at 225 °C in a high-pressure oxygen atmosphere (Fig. 2a, b; Craw 2006). Ore concentrate, with added crushed limestone and water, passes as a slurry through the autoclave with a residence time of 45–70 min (Fig. 2a, b). The residence time has increased slightly since 2016 as lower volumes of available concentrate have allowed slower throughput and more complete oxidation. There are three compartments in the autoclave with the first one, being larger, having two designated sub-compartments (Fig. 2a, b). The walls of the autoclave are lined with refractory tiles that are held in place with Pb-bearing grout (Fig. 2b) and minor Pb contamination of the ore slurry occurs at times, especially after a maintenance session has renewed the grout. Much of the sulfide oxidation occurs in the first two sub-compartments although almost-complete oxidation of some components, especially Fe, does not occur until the third compartment. The Macraes mine concentrate has constituted most of the feed to the autoclave, with Reefton concentrate forming 30–40% of the feed (50–60 kt/year) from 2007 to 2016. Reefton concentrate had higher sulfide content than Macraes concentrate and was treated separately from Macraes concentrate, for periods of ≈ 4 days each.

Mineral scales form precipitates from the oxidising concentrate slurry on the inside of the autoclave, on the walls, compartment separation barriers, and the agitators (Fig. 2b; Craw 2006; Kerr et al. 2015a). The scales are manually cleaned out of the autoclave four times a year, and the minerals provide a useful indication of the progression of oxidation through the autoclave (Craw 2006). Typically, scales from sub-compartments 1A and 1B are composed of ferrous sulfates, calcium sulfates, and arsenous oxides, while scales in compartments 2 and 3 are primarily composed of jarosite, hematite, and ferric arsenate.

The autoclave produces highly acidic discharge waters (pH ≈ 1; Craw 2006), and by then 80% of the available iron in ore concentrate has been oxidised. The discharge waters contain jarosite, hematite, ferric arsenate, and abundant fine-grained amorphous As-bearing ferric oxyhydroxide material (designated HFO + As herein; Fig. 2c, d; Craw 2006). The acid waters are neutralised with flotation tailings (pH ≈ 8) and thickened high-density solids are further neutralised with lime for cyanidation at pH > 10. After cyanidation, residual cyanide is oxidised (INCO process; Breuer and Hewitt 2019) and tailings are discharged into the mixed tailings impoundment with flotation tailings (Fig. 1b, 2c).

Methods

This study used archived water data taken as part of routine environmental monitoring by the mining company at the Macraes and Reefton sites. For this study, water data were selected for the Reefton tailings impoundment and the water treatment discharge at the processing plant (Fig. 1c), and from both tailings impoundments at Macraes (Fig. 1b). Water samples were collected and analysed on a 1–3 monthly schedule (Craw and Pope 2017; Druzbicka and Craw 2013; Weightman et al. 2020). Samples were filtered at the laboratories (0.45 µm), and the analytical techniques used were in accord with methods of American Public Health Association (APHA 2005), mainly by ICP-OES or ICP-MS. Analyses of As and Sb contents were conducted on all waters at the Reefton site. Arsenic was analysed in all waters at Macraes,

but Sb analyses were obtained only sporadically during the period when Reefton concentrate was being processed.

Samples of autoclave scales were analysed using an X-ray diffractometer (XRD) with Cu Kα radiation on a PANalytical X'Pert Pro MPD PW3040/60 instrument housed in the Geology Department, University of Otago. Diffraction patterns were analysed digitally with PANalytical High Score software package. Many of the minerals in the scales, as determined by XRD at room temperature, were variably hydrated species and it is not known if these species formed within the autoclave, during the cooling and sampling period, or after crushing and preparation in the XRD laboratory. Hence, we mainly refer to these minerals by generic names, rather than specific XRD identities. For example, ferrous sulphates are common in the first autoclave compartment, and these were identified by XRD as hydrated species szomolnokite ($FeSO_4 \cdot H_2O$) and rozenite ($FeSO_4 \cdot 4H_2O$). Similarly, anhydrite ($CaSO_4$) and gypsum ($CaSO_4 \cdot 2H_2O$) are common scale minerals, as are ferric arsenate ($FeAsO_4$) and scorodite ($FeAsO_4 \cdot 2H_2O$).

Fifteen sets (15–19 samples per set) of scale samples gathered from the autoclave were selected for the period 2013–2019, to overlap the cessation of Reefton concentrate addition to the processing system in 2016. Bulk compositions of the autoclave scale samples were determined for Fe, As, Sb, and Pb with an Olympus Innov-X Vanta field portable X-ray fluorescence instrument (fp-XRF) with a rhodium (Rh) anode 50 kV X-ray tube. Measurements were obtained with a 30-s acquisition time on dry crushed (< 50 µm) material. The fp-XRF instrument measures from a window area of ≈ 1 cm^2 and the scale minerals are intimately intergrown at the submillimetre scale and are inhomogeneous, so the bulk compositional data give only broad generalisations of differences among samples. Further, the fp-XRF results on loosely packed powders are inherently imprecise, and the results are only semiquantitative. Results from fp-XRF for similar samples with high levels of As and Sb are typically within 10–20% (relative) of values obtained from more precise laboratory instruments (Druzbicka and Craw 2015; Kerr and Craw 2020). The practical detection limit for metalloids with the fp-XRF is ≈ 50 mg/kg for the material examined in this study.

Based on bulk fp-XRF analyses, relatively Sb-rich scale samples were selected for further detailed mineralogical study from the sample set collected in February 2016. Scanning electron microscopy (SEM) with an energy dispersive spectroscopy (EDS) analytical attachment was used to examine these selected precipitates. This was done on a Zeiss Sigma VP (variable pressure) SEM fitted with a HKL INCA Premium Synergy Integrated EDS system at the Otago Micro and Nano Scale Imaging Centre (OMNI), University of Otago. Samples were carbon-coated prior to examination. Autoclave chip samples for SEM analysis were either mounted with carbon tape and carbon paint on aluminium stubs or mounted in resin briquettes and polished. Neither of these preparation techniques avoided persistence of rough surfaces for examination, as scale minerals are readily fragmented, plucked, and locally corroded during preparation. These rough surfaces inhibited EDS analytical precision, and detection limits for Sb and As were ≈ 0.5–1 wt%. Further, many intergrowths of scale minerals were finer grained than the EDS analytical beam size of ≈ 3 µm, so composite analyses resulted from these intergrowths.

Results

Reefton Mine Waters

Tailings from the sulfide concentration process were discharged as a slurry into the large tailings impoundment at Reefton (Fig. 1c). Tailings decant waters were then pumped back to the processing plant for recycling through the system (Fig. 1c), along with other mine waters. The site receives abundant and regular rainfall (> 2000 mm/year) and water was in excess, so some mine water was diluted and discharged from the site (Fig. 1c) into an adjacent river where further dilution occurred. However, treatment of discharge water was required to lower metalloid concentrations, especially Sb, which commonly exceeded the regulatory limit of 1 mg/L in the tailings (Fig. 3a; Druzbicka and Craw 2013). This treatment was done at the processing plant with adsorption to ferric oxyhydroxide and the solid precipitates were removed via filtration and settling in engineered ponds. Nevertheless, waters leaving the mine site have had Sb fluxes up to 100 mg/sec at times, during the early stages of mining (Druzbicka and Craw 2013).

Crushing, agitation, and concentration of the sulfide-bearing ore resulted in elevation of dissolved metalloid concentrations to between 0.1 and 10 mg/L in tailings waters for most of the life of the Reefton mine (Fig. 3a). The dissolved Sb concentrations were similar to, or slightly higher than, the dissolved As concentrations (Fig. 3a). In contrast, the treated waters had distinctly lower As concentrations than the tailings waters but similar Sb concentrations (Fig. 3b). The tailings waters were consistently alkaline, with pH typically between 7 and 8.5 (Fig. 4a), reflecting abundant carbonate contents in the ore, and recycling of the mine waters ensured that the pH generally rose during the life of the mine (Fig. 4a). Similarly, the treated waters were generally alkaline (pH 7 to 8.5) with the same general trend in increased pH over the life of the mine (Fig. 4a).

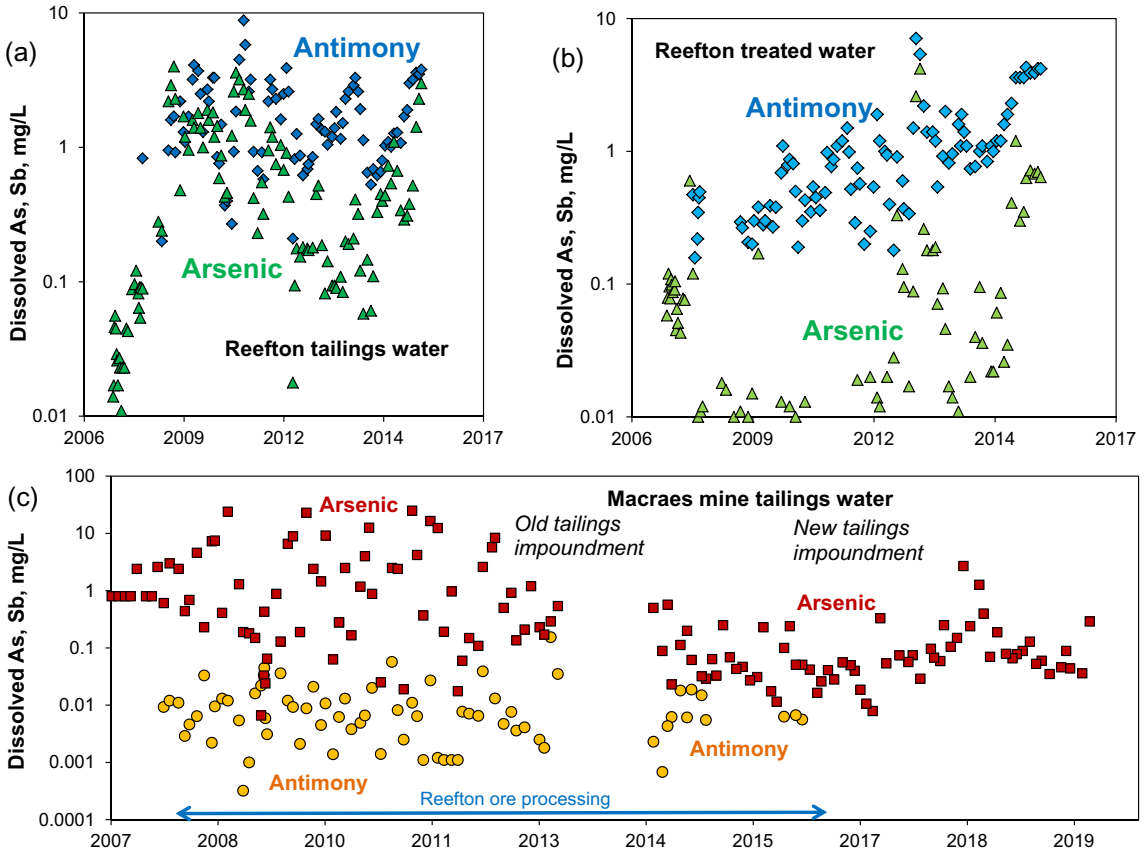

Fig. 3 Comparisons of time series of As and Sb concentrations in mine waters at Reefton and Macraes sites, as in Fig. 1b, c. **a** Tailings decant water at Reefton. **b** Treated mine waters at Reefton. **c** Tailings decant water at Macraes, in old impoundment (left) and new impoundment (right)

Macraes Tailings Waters

The Macraes site has a relatively dry climate, with ≈ 600 mm annual rainfall and ≈ 700 mm/year potential evaporation, and so the site has a water deficit. Hence, most mine processing waters are recycled, with no discharges from the site (Fig. 1b). Tailings from the flotation stage and oxidised and cyanided ore concentrate are discharged as separate slurries that mix in the tailings impoundment. The combined decant water is then pumped back to the processing plant for recycling (Fig. 1b). An old tailings impoundment was decommissioned and a new one commissioned at the site in 2013 (Fig. 1b) during the period of Reefton concentrate importation.

The dissolved As concentrations in Macraes tailings waters were typically between 0.1 and 10 mg/L in the old tailings impoundment, with occasional elevation to > 20 mg/L (Fig. 3c). The dissolved As concentrations generally declined during the transition to the new tailings impoundment and dissolved As has mostly remained near 0.1 mg/L (Fig. 3c). Dissolved Sb was consistently < 0.1 mg/L, and commonly < 0.01 mg/L, throughout the period of Reefton ore processing (Fig. 3c). The distinctly lower Sb than As at Macraes contrasts strongly with the compositions of Reefton mine waters (Fig. 4b). The pH of the Macraes tailings waters has evolved from moderately acidic in the old tailings impoundment to alkaline (pH 8) in the new tailings impoundment (Fig. 4c). This latter pH rise has occurred because of more complete oxidation of ferric iron in the autoclave since 2016 (above).

Autoclave Scale Compositions

The scale deposits can be > 10 cm thick, and are typically mineralogically layered, with individual layers 0.1–10 mm thick (Fig. 5a, b). Layers typically consist of one to three minerals, most of which form well-defined crystals (Fig. 5a, b) that can be up to 10 mm in length. Frequent repetition of layering is common, with the minerals in the different layers reflecting the degree of oxidation within each part of the autoclave (Fig. 2b). However, the degree of oxidation varied with time at some positions, so that juxtaposition of oxidised and less oxidised minerals is common, especially in compartment 1 (Figs. 2b; 5a, b). In addition, there has been some superimposition of mineral growth along veins and fractures that crosscut the early-formed layers (Fig. 5b).

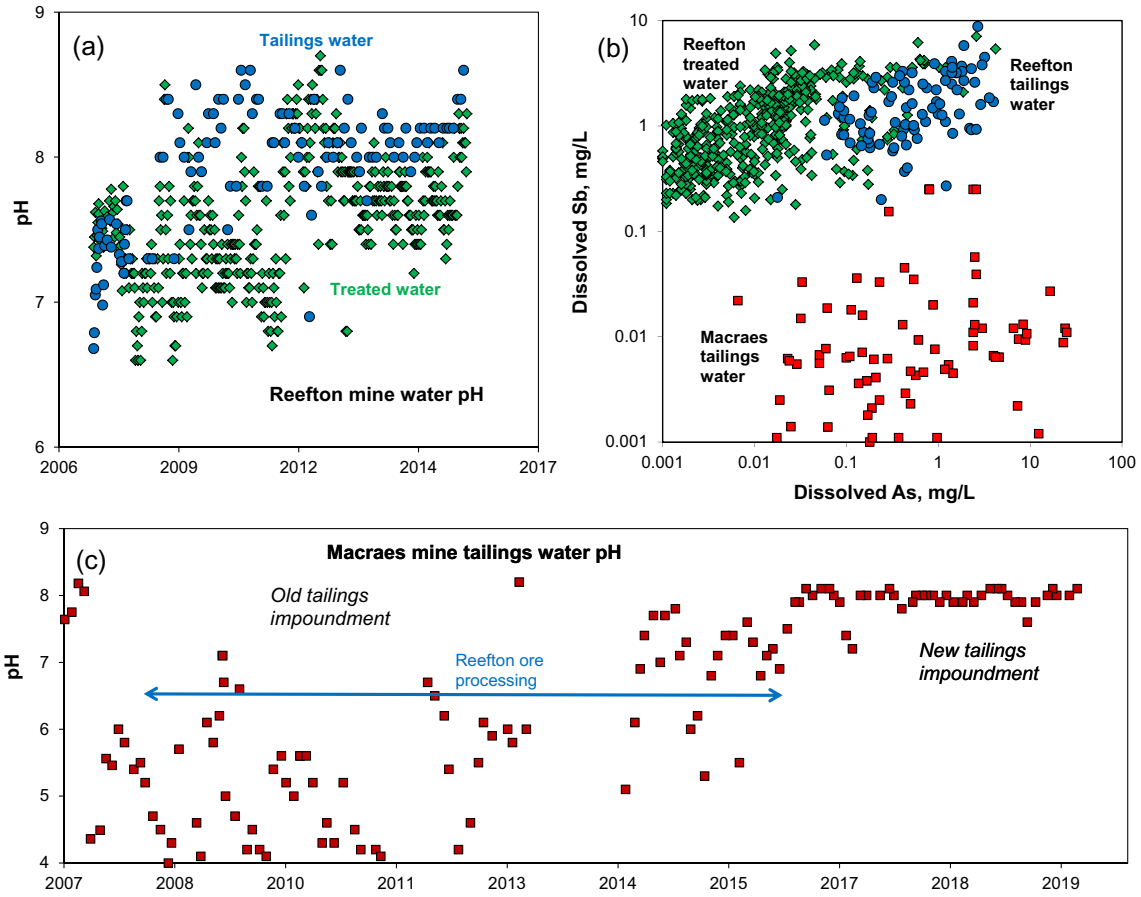

Fig. 4 Comparison of mine water compositions at Reefton and Macraes sites. **a** Time series of pH for tailings and treated waters at Reefton. **b** Comparison of As versus Sb concentrations of mine waters at Reefton and Macraes. **c** Time series of pH for tailings waters at Macraes spanning the period of Reefton concentrate addition

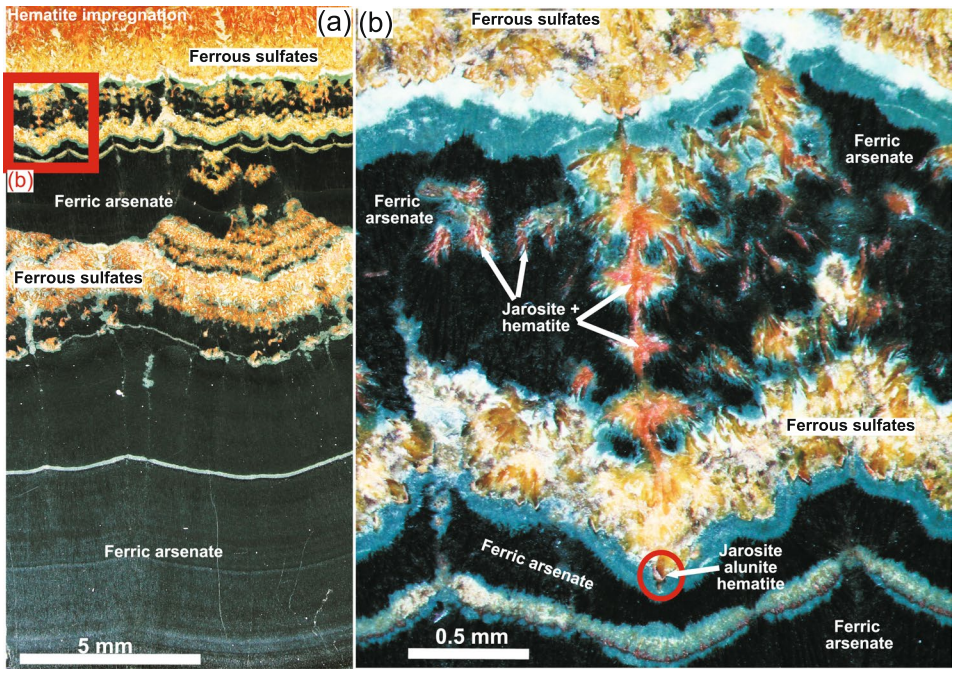

Fig. 5 Photograph of a polished block of typical autoclave scale from compartment 1B of the Macraes autoclave, showing the principal mineralogy and textures in the main stage of oxidation. **a** General view of the layering. **b** Close view of layering with late-stage cross-cutting textures

The fp-XRF analyses show that most elements have broadly consistent concentrations over time in the scale sets examined in this study. The most abundant elements were Fe (average 21 wt%; Fig. 6a, b), As (average 5.6 wt%; Fig. 6c, d), S (average 4.1 wt%), Ca (average 1.7 wt%), and K (average 1.2 wt%). The Fe concentrations were broadly similar through the autoclave, with a general increase in concentration towards the more oxidised end (Fig. 6b). Lead contamination from the walls of the autoclave (Fig. 2b) was ≈ 2 wt% in some scales, and locally reached to 16 wt% in the scales collected from compartment 1B in February 2016, after a major refurbishment of the autoclave. Lead extraction from the walls was enhanced by the Reefton concentrate, which had higher S and generated more acid than Macraes concentrate.

Antimony in Scales

Concentrations of Sb in crushed scale samples ranged from < 1000 mg/kg to ≈ 3 wt% during the period of Reefton concentrate addition, and then decreased after 2016 to remain consistently < 2000 mg/kg (Fig. 6e). Elevated Sb concentrations from the Reefton concentrate were confined mainly to compartments 1A and 1B, with some minor spread into compartment 2 of the autoclave (Fig. 6e, f). Similarly, As concentrations were highest in scale samples from compartments 1A and 1B and decreased markedly towards the more oxidised end of the autoclave (Fig. 6d).

One XRD pattern from a compartment 1B scale in 2015 had small peaks that indicate the presence of a ferric antimonate mineral, tripuhyite. Unfortunately, overlaps with XRD peaks from the more abundant minerals made this identification tentative, but this prompted closer examination

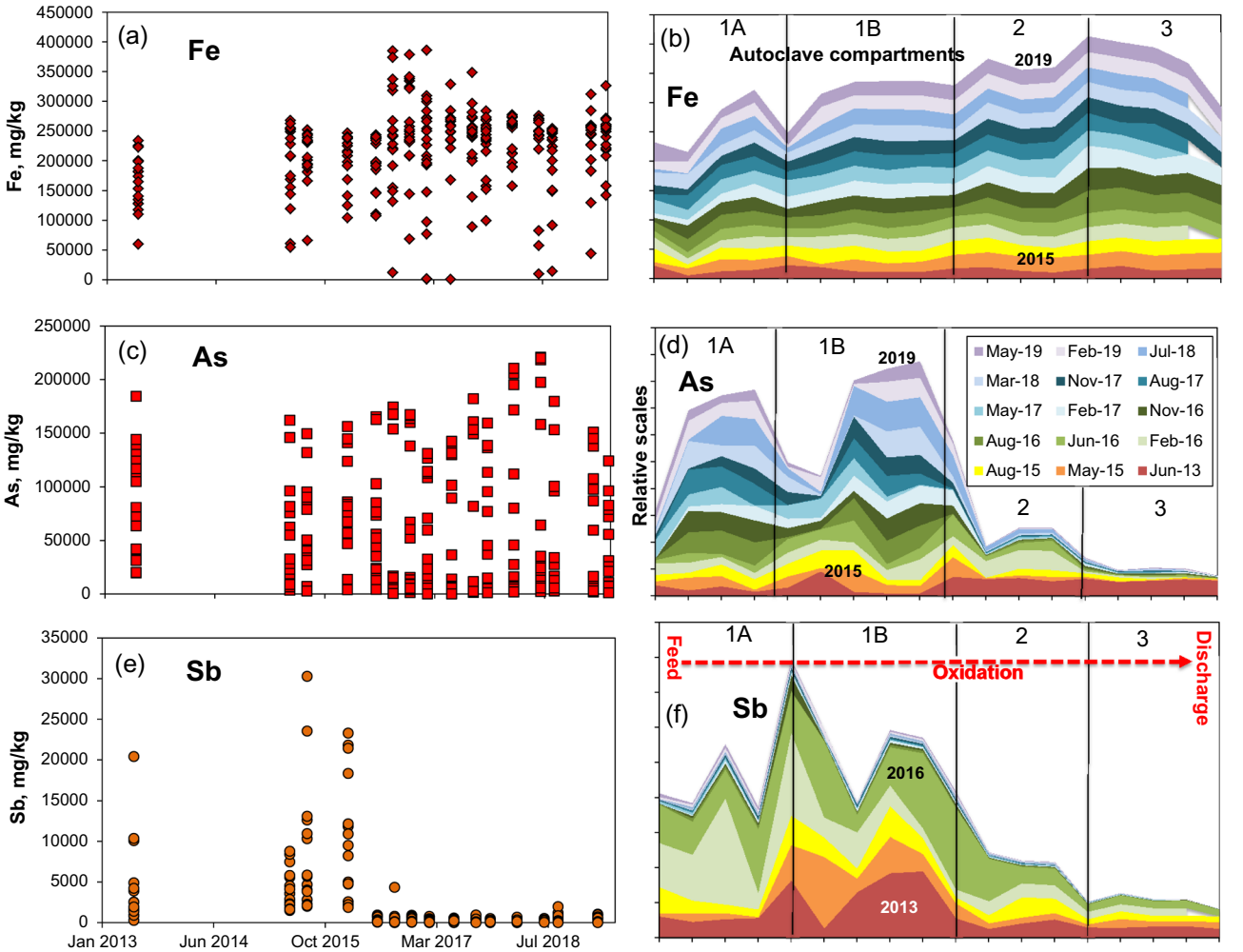

Fig. 6 Principal metal contents, from fp-XRF analyses, of 15 sets of autoclave scales collected between 2013 and 2019 across the transition from Reefton concentrate addition to Macraes concentrate only. **a** Fe concentrations in each set. **b** Relative amounts of Fe at different stages through the autoclave, stacked from oldest (bottom) to youngest (top). **c** As concentrations. **d** Stacked relative As contents through the autoclave. **e** Sb concentrations. **f** Stacked relative Sb contents through the autoclave

of similar material by XRD-EDS. A solid chip of scale collected from compartment 1B in February 2016 had ≈ 3 wt% Sb, and this sample was selected for more detailed examination in a polished block (Fig. 7a–c). This specimen contained distinctive yellow layers within grey crystalline ferrous sulfates (Figs. 7a; 8a, b). The scale set from which this specimen was selected in compartment 1 also included arsenous oxide (claudetite), ferric arsenate, and hematite (Fig. 8a, b).

SEM–EDS analyses showed that the yellow layers contain the highest Sb concentrations and the material with high Sb concentrations is intergrown with the Pb sulfate mineral anglesite (Fig. 7b, c). The Sb in the scale occurs as Fe-Sb-As-O compounds with two different textures: apparently well-defined crystals with consistent compositions and fine-grained intergrowths with highly variable compositions (Figs. 7b, c; 8b). The well-defined crystals have compositions that are intermediate between tripuhyite and ferric arsenate (Fig. 8c). The coexisting fine grained material has a wide range of compositions and includes some end-member ferric arsenate (Fig. 8b, c).

Discussion

Adsorption of As and Sb to Ferric Oxyhydroxide (HFO)

Adsorption of dissolved As, especially arsenate ions, to HFO is a well-established phenomenon and is responsible for extraction of As from waters around many mine sites (Bowell 1994; Mohan and Pitman 2007; Ritchie et al. 2013; Roddick-Lanzilotta et al. 2002; Swedlund et al. 2015; Waychunas et al. 1993; Yin et al. 2019). This process was the basis for extraction of As from Reefton mine waters, where the active water treatment system created HFO from added ferric chloride (Milham and Craw 2009; Muller et al. 2015). Treatment typically decreased dissolved As from > 1 to < 0.1 mg/L and as low as 0.01 mg/L at times (Figs. 3a, b; 9a). Arsenic adsorption to HFO is most effective under weakly acidic to circumneutral conditions (Bowell 1994; Jain et al. 1999; Swedlund et al. 2015) but was effective at Reefton at relatively high pH (6–8.5; Figs. 4a; 9a). Arsenate ions are adsorbed to the HFO surface by a bidentate mechanism (Fig. 9b; Muller et al. 2015; Roddick-Lanzilotta et al. 2002; Yin et al. 2019).

Antimony can also be adsorbed to HFO under similar conditions (Druzbicka and Craw 2015; Guo et al. 2014; McComb et al. 2007; Vithanage et al. 2013). However, antimonate ions form unidentate ligands for adsorption to HFO and these links are weaker than those of bidentate arsenate (Muller et al. 2015). Hence, where there is competition between arsenate and antimonate ions for adsorption sites, arsenate ions prevail and displace antimonate, especially at circumneutral pH (Fig. 9b; Muller et al. 2015). This adsorption competition resulted in less effective removal of Sb compared to As in the Reefton mine water treatment system and possibly in the tailings waters as well (Figs. 3a; 4b), leading to Reefton mine waters with dissolved Sb > As (Fig. 9a, b). Persistence of dissolved Sb > As was also noted in laboratory experiments on Reefton ore samples by Kerr et al. (2015b).

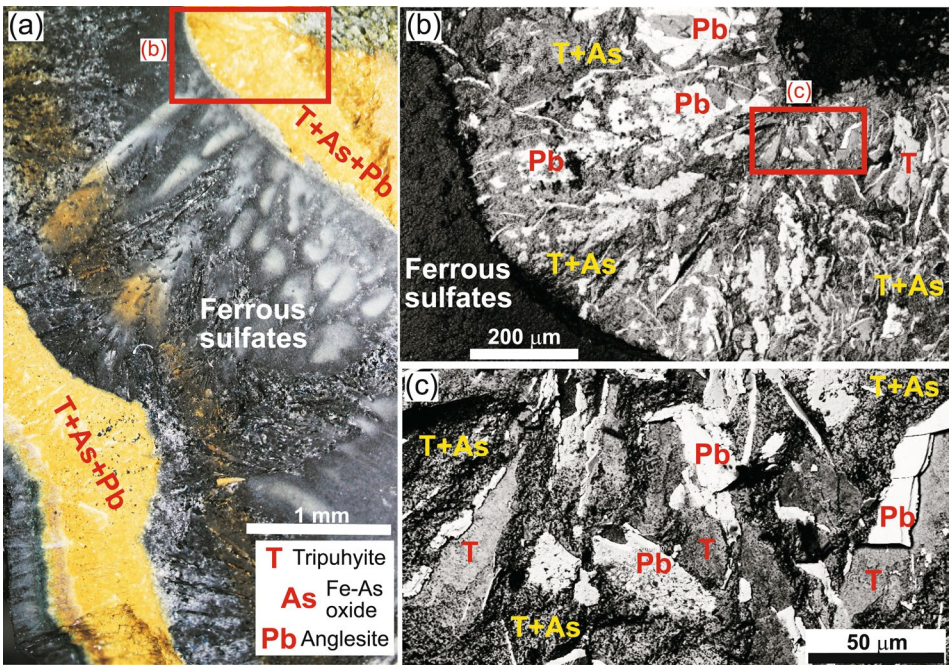

Fig. 7 Mineralogy in a polished block of relatively Sb-rich autoclave scale from compartment 1B of the Macraes autoclave from February 2016 (Fig. 6f). **a** Photograph of the block. **b** SEM image of a Sb-rich layer, as in **a**. **c** Detailed SEM image (as in **b**) of Sb-bearing mineral material

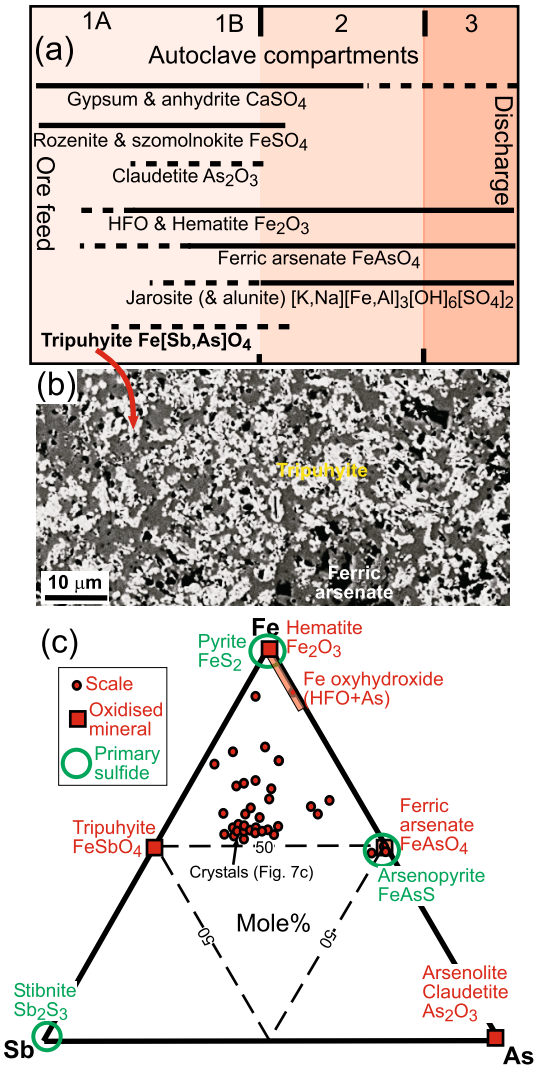

Fig. 8 Mineralogical data for the February 2016 set of autoclave scales. **a** Mineralogical variation through the autoclave, showing the relative position of tripuhyite-bearing scales (as in Fig. 7). **b** SEM image of intergrown tripuhyite and ferric arsenate. **c** SEM–EDS analyses of As-bearing ferric antimonate (tripuhyite) crystals and associated fine grained material in the scales in Fig. 7b, c

Adsorption of As to HFO has been a major factor in removing dissolved As from mine waters at the Macraes mine, both in the processing plant discharge waters to tailings and in tailings waters seeping through the tailings impoundment structure (Craw and Pope 2017; Roddick-Lanzilotta et al. 2002). At least some of the As associated with HFO particles discharged from the autoclave to the tailings (Fig. 2c, d) is likely to be adsorbed (Craw and Pope 2017). However, direct precipitation of ferric arsenate is also an important phenomenon in the autoclave (Fig. 5). Slower autoclave throughput, with associated increased oxidation efficiency, since 2016 may have been responsible for enhanced precipitation of ferric arsenate and less dissolved As in the tailings waters (Fig. 3c).

Tripuhyite in Autoclave Scales

The yellow colour and crystalline form of the ferric antimonate mineral observed in this study (Fig. 7a) is similar to descriptions of tripuhyite recorded by Kossoff et al. (2015) and Multani et al. (2017). The intergrown nature of ferric antimonate and ferric arsenate in the scales limits confidence in the SEM–EDS mineral analyses as representing single minerals. Hence, it is not clear if the ferric antimonate crystals contain As in solid solution or as a physical mixture with ferric arsenate. However, the generally consistent compositions of the crystals (Fig. 8b) compared to the fine-grained surrounding material that clearly is physically mixed (Fig. 7c; 8c) supports a solid solution interpretation. In low-temperature experiments generating ferric arsenate in the presence of dissolved Sb, Kossoff et al. (2015) found that despite some chemical similarities, Sb does not substitute into ferric arsenate. However, at the high temperatures of the autoclave process, the substitution of As for Sb in tripuhyite may be possible, and we infer that the crystals and perhaps much of the fine grained surrounding material in Fig. 7c are As-bearing tripuhyite (Fig. 9c, d).

Irrespective of the exact mineral formed, autoclave processing appears to have caused rapid and effective Sb oxidation in parallel with As oxidation (Fig. 6d, f). Precipitation of ferric antimonate as a tripuhyite-like mineral during this oxidation has assisted in removal of dissolved Sb from the oxidising ore slurry (Fig. 9c, d). Consequently, dissolved Sb concentrations remained low (0.001–0.1 mg/L) in tailings waters discharged from the Macraes processing plant throughout the period of addition of stibnite-bearing Reefton concentrate (Fig. 3c; 4b). Formation of ferric antimonate precipitates in the autoclave have therefore been responsible for dissolved Sb < As in the Macraes tailings waters, in strong contrast to many of the Reefton mine waters where Sb > As (Fig. 4b; Fig. 9a–d; Leverett et al. 2012).

The mineral scales in the autoclave provide a snapshot of the oxidation and precipitation processes within the autoclave, but the Sb-bearing scales are volumetrically minor. Most of the Sb that precipitated as ferric antimonate will have been discharged with the more abundant HFO + As, ferric arsenate, and jarosite into the downstream gold-saving system and then into the tailings. Since the solid Sb-bearing residues are so volumetrically minor, finding this material in a tailings sample (cf Fig. 2c, d) is highly unlikely. Nevertheless, the presence of tripuhyite, a relatively insoluble mineral (Leverett et al. 2012; Majzlan et al. 2016) in the tailings, ensures that Sb is unlikely to be an environmental issue at the site.

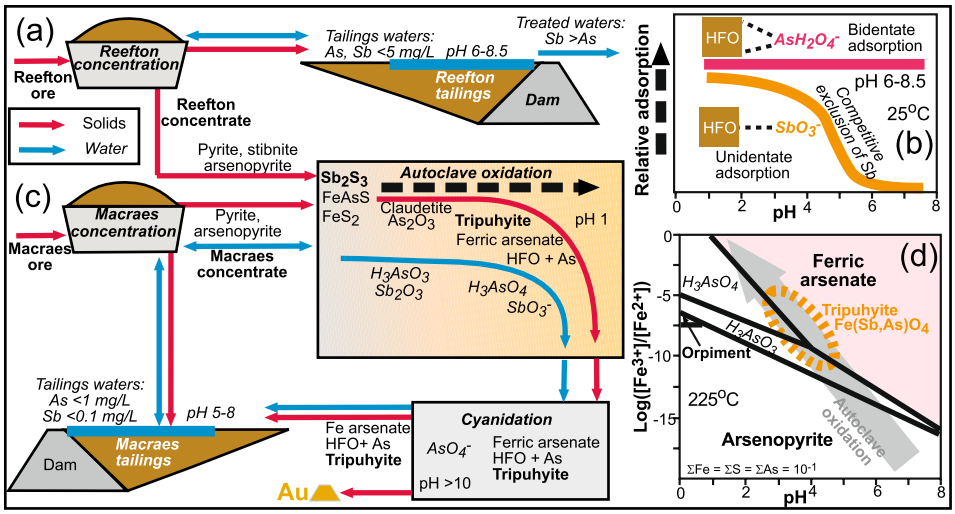

Fig. 9 Cartoon summary of the mineral processing systems at Reefton and Macraes sites, with As and Sb mineralogy and mine water compositions. **a** Reefton site. **b** Macraes site. **c** Relative adsorption of As and Sb at Reefton site (generalised from Muller et al. 2015). **d** Autoclave oxidation products at Macraes. Modified from Craw (2006)

Summary and Conclusions

Ore at the Reefton orogenic gold mine in southern New Zealand is refractory, with gold encapsulated in sulfide minerals. A sulfide concentrate that included pyrite, arsenopyrite, and stibnite was produced at the site between 2007 and 2016. Consequently, tailings waters contained dissolved arsenic (As) and antimony (Sb) up to 5 mg/L at alkaline pH (7–8.5). Treatment of mine waters with ferric oxyhydroxide (HFO) formed from added ferric chloride extracted As down to < 0.1 mg/L. However, dissolved Sb remained elevated because unidentate antimonate ligands on the HFO adsorption surfaces were outcompeted by bidentate arsenate ions.

The Macraes orogenic gold mine, which opened in 1990, also has refractory ore, and a sulfide concentrate from this ore is oxidised with a pressure oxidation autoclave (225 °C). The Macraes ore concentrate contains pyrite and arsenopyrite but no stibnite, and has low Sb content (Fig. 9c), The autoclave discharges an oxidised concentrate that includes ferric arsenate, jarosite, and HFO + As, and this material passes through a cyanidation plant to extract gold before being discarded in a tailings impoundment (Fig. 9c) All of the Reefton sulfide concentrate was transported 700 km to Macraes and processed through the autoclave in parallel with the Macraes concentrate between 2007 and 2016.

Mineral scales formed on the inside of the autoclave record the progressive oxidation process (Fig. 9c). Stibnite oxidation occurred rapidly in the first compartment of the autoclave, and mineral scales formed at that stage contained ferric antimonate, probably As-bearing tripuhyite, Fe[Sb,As]O_4. This mineral was accompanied by ferric arsenate in the autoclave (Fig. 9d). There is not a complete solid solution between ferric antimonate and ferric arsenate. Incomplete oxidation of Fe at this early stage also allowed precipitation of ferrous sulphates with the tripuhyite.

The Macraes tailings waters had pH < 7 when Fe oxidation was incomplete during the time of addition of Reefton concentrate, and this rose to pH 8 after that addition ceased. Dissolved Sb in the Macraes tailings waters remained < 0.1 mg/L throughout the period of Reefton concentrate addition (Fig. 9c). At the same time, dissolved As decreased from > 5 to < 1 mg/L, and then decreased further (to ≈ 0.1 mg/L) over the transition from Reefton-bearing ore feed to Macraes only ore-feed.

Tripuhyite is a mineral with low solubility under surface conditions, so formation of tripuhyite in the high-temperature autoclave has stabilised Sb in the Macraes tailings. Hence, tailings waters have dissolved Sb < As, since the autoclave yields As compounds more soluble than tripuhyite. This situation is in strong contrast to the low-temperature processes at Reefton where dissolved Sb > As. Lowering of dissolved Sb at that site relied partially on dilution by surrounding waters in a wet climate.

Acknowledgements This research was funded by the University of Otago and Oceana Gold Ltd. and logistical support and samples were provided by Oceana Gold personnel. Brent Pooley created excellent polished sections and Marianne Negrini provided expert assistance with SEM observations at the Otago Micro and Nano Scale Imaging Centre (OMNI), University of Otago. Three journal referees provided useful pointers for revision of the ms.

References

APHA (2005) Standard methods for the examination of water and wastewater, 21st edn. American Public Health Association, Washington, DC

Ashley P, Craw D, Graham B, Chappell D (2003) Environmental mobility of antimony around mesothermal stibnite deposits, New South Wales, Australia and southern New Zealand. J Geochem Explor 77:1–14

Bowell R (1994) Sorption of arsenic by iron oxides and oxyhydroxides in soils. Appl Geochem 9:279–286

Bowell RJ, Craw D (2014) Chapter 11. The management of arsenic in the mining industry. In: Bowell RJ, Alpers C, Jamieson H,

Nordstrom DK, Majzlan J (eds) arsenic, vol 79. Mineralogical Society of America Reviews in Mineralogy, pp 507–532
Breuer PL, Hewitt DM (2019) INCO cyanide destruction insights from plant reviews and laboratory evaluations. Trans Inst Min Metall 129:104–113
Craw D (2006) Pressure-oxidation autoclave as an analogue for acid–sulphate alteration in epithermal systems. Miner Deposita 41:357–368
Craw D, MacKenzie D (2016) Macraes gold deposit, New Zealand. SpringerBriefs in World Mineral Deposits, p 130 (**ISBN 978-3-319-35158-2**)
Craw D, Pope J (2017) Time-series monitoring of water-rock interactions in mine wastes, Macraes gold mine, New Zealand. NZ J Geol Geophys 60:159–175
Druzbicka J, Craw D (2013) Evolving metalloid signatures in waters draining from a mined orogenic gold deposit, New Zealand. Appl Geochem 31:251–264
Druzbicka J, Craw D (2015) Metalloid attenuation from runoff waters at an historic orogenic gold mine, New Zealand. Mine Water Environ 34:417–429
Fawcett SE, Jamieson HE, Nordstrom DK, McCleskey R (2015) Arsenic and antimony geochemistry of mine wastes, associated waters and sediments at the Giant Mine Yellowknife, Northwest Territories, Canada. Appl Geochem 62:3–17
Filella M, Williams PA, Belzile NJEC (2009) Antimony in the environment: knowns and unknowns. Environ Chem 6:95–105
Fleming C, Metallurgy (2010) Basic iron sulfate—a potential killer in the processing of refractory gold concentrates by pressure oxidation. Miner Metall Proc 27:81–88
Guo X, Wu Z, He M, Meng X, Jin M, Qiu N, Zhang J (2014) Adsorption of antimony onto iron oxyhydroxides: adsorption behaviour and surface structure. J Hazard Mater 276:339–345
Jain A, Raven K, Loeppert R (1999) Arsenite and arsenate adsorption on ferrihydrite: surface charge reduction and net OH-release stoichiometry. Environ Sci Technol 33(8):1179–1184
Karimian N, Johnston SG, Burton ED (2017) Antimony and arsenic behavior during Fe (II)-induced transformation of jarosite. Environ Sci Technol 51:4259–4268
Kerr G, Craw D (2020) Arsenic residues from historic gold extraction, Snowy River, Westland, New Zealand. NZ J Geol Geophys 63 **(in press)**
Kerr G, Druzbicka J, Lilly K, Craw D (2015a) Jarosite solid solution associated with arsenic-rich mine waters, Macraes mine, New Zealand. Mine Water Environ 34:364–374
Kerr G, Pope J, Trumm D, Craw D (2015b) Experimental metalloid mobilisation from a New Zealand orogenic gold deposit. Mine Water Environ 34:404–416
Kossoff D, Welch MD, Hudson-Edwards K (2015) Scorodite precipitation in the presence of antimony. Chem Geol 406:1–9
La Brooy S, Linge H, Walker G (1994) Review of gold extraction from ores. Miner Eng 7:1213–1241
Langmuir D, Mahoney J, Rowson J (2006) Solubility products of amorphous ferric arsenate and crystalline scorodite ($FeAsO_4$–$2H_2O$) and their application to arsenic behavior in buried mine tailings. Geochim Cosmochim Acta 70(12):2942–2956
Leverett P, Reynolds JK, Roper AJ, Williams P (2012) Tripuhyite and schafarzikite: two of the ultimate sinks for antimony in the natural environment. Mineral Mag 76:891–902
Majzlan J, Lalinska B, Chovan M, Blass U, Brecht B, Gottlicher J, Steininger R, Hug K, Ziegler S, Gescher J (2011) A mineralogical, geochemical, and microbiological assessment of the antimony- and arsenic-rich neutral mine drainage tailings near Pezinok, Slovakia. Am Mineral 96:1–13
Majzlan J, Drahota P, Filippi M (2015) Parageneses and crystal chemistry of arsenic minerals. In: Bowell RJ, Alpers C, Jamieson H, Nordstrom DK, Majzlan J (eds) Arsenic, vol 79. Mineralogical Society of America Reviews in Mineralogy, pp 17–184
Majzlan J, Stevko M, Lanczos T (2016) Soluble secondary minerals of antimony in Pezinok and Kremnica (Slovakia) and the question of mobility or immobility of antimony in mine waters. Environ Chem 13:927–935
McComb KA, Craw D, McQuillan AJ (2007) ATR-IR spectroscopic study of antimonate adsorption to iron oxide. Langmuir 23:12125–12130
Maher W (2009) Antimony in the environment—the new global puzzle. Environ Chem 6:93–94
Milham L, Craw D (2009) Antimony mobilization through two contrasting gold ore processing systems, New Zealand. Mine Water Environ 28:136–145
Mohan D, Pittman CR (2007) Arsenic removal from water/wastewater using adsorbents—a critical review. J Hazard Mater 142:1–53
Muller T, Craw D, McQuillan AJ (2015) Arsenate and antimonate adsorption competition on 6-line ferrihydrite monitored by infrared spectroscopy. Appl Geochem 61:224–232
Multani RS, Feldmann T, Demopoulos G (2017) Removal of antimony from concentrated solutions with focus on tripuhyite ($FeSbO_4$) synthesis, characterization and stability. Hydrometallurgy 169:263–274
Paktunc D, Majzlan J, Palatinus L, Dutrizac J, Klementová M, Poirier G (2013) Characterization of ferric arsenate-sulfate compounds: Implications for arsenic control in refractory gold processing residues. Am Miner 98:554–565
Radkova AB, Jamieson H, Bronislava L-V, Majzlan J, Stevko M, Chovan M (2017) Mineralogical controls on antimony and arsenic mobility during tetrahedrite-tennantite weathering at historic mine sites Spania Dolina-Piesky and Ľubietova-Svatodusna, Slovakia. Am Miner 102:1091–1100
Radkova AB, Jamieson HE, Campbell KM (2020) Antimony mobility during the early stages of stibnite weathering in tailings at the Beaver Brook Sb deposit Newfoundland. Appl Geochem 115:104528
Ritchie VJ, Ilgen AG, Mueller SH, Trainor TP, Goldfarb RJ (2013) Mobility and chemical fate of antimony and arsenic in historic mining environments of the Kantishna Hills district, Denali National Park and Preserve, Alaska. Chem Geol 335:172–188
Riveros P, Dutrizac J, Spencer P (2001) Arsenic disposal practices in the metallurgical industry. Can Metall Q 40:395–420
Roddick-Lanzilotta AJ, McQuillan AJ, Craw D (2002) Infrared spectroscopic characterisation of arsenate (V) ion adsorption from mine waters, Macraes, New Zealand. Appl Geochem 17:445–454
Swedlund PJ, Holtkamp H, Song Y, Daughney CJ (2015) Arsenate–ferrihydrite systems from minutes to months: a macroscopic and IR spectroscopic study of an elusive equilibrium. Environ Sci Technol 48:2759–2765
Vithanage M, Rajapaksha AU, Dou X, Bolan NS, Yang JE, Ok YS (2013) Surface complexation modelling and spectroscopic evidence of antimony adsorption on iron-rich-red earth soils. J Colloid Interface Sci 406:217–224
Waychunas GA, Rea BA, Fuller CC, Davis JA (1993) Surface chemistry of ferrihydrite: part 1. EXAFS studies of the geometry of coprecipitated and adsorbed arsenate. Geochim Cosmochim Acta 57:2251–2269
Weightman E, Craw D, Rufaut C, Kerr G, Scott J (2020) Chemical evolution and evaporation of shallow groundwaters discharging from a gold mine, southern New Zealand. Appl Geochem 122:104766 (**on-line Sept 2020**)
Yin Z, Lutzenkirchen J, Finck N, Celaries N, Dardenne K, Hansen H (2019) Adsorption of arsenic(V) onto single sheet iron oxide: x-ray absorption fine structure and surface complexation. J Colloid Interface Sci 554:433–443